Journal of Geochemical Exploration 165 (2016) 189–198

Contents lists available at ScienceDirect

Journal of Geochemical Exploration

journal homepage: www.elsevier.com/locate/gexplo

Implications for the origin of secondary sylvite from a simulation of carnallite dissolution

Huai De Cheng *, Qing Yu Hai, Hai Zhou Ma, Xi Ying Zhang, Qi Liang Tang, Qi Shun Fan, Yong Shou Li, Wei Liang Miao

Qinghai Institute of Salt Lakes, Chinese Academy of Sciences, No 18 Xinning Road, Xi'ning, Qinghai 810008, China

ARTICLE INFO

Article history:
Received 1 September 2015
Revised 10 March 2016
Accepted 28 March 2016
Available online 31 March 2016

Keywords:
Carnallite
Flotation separation
Leaching dissolution
Potash
Secondary sylvite

ABSTRACT

The relationship between sylvinite (KCl + NaCl) and carnallite ($KCl \cdot MgCl_2 \cdot 6H_2O$) is important in potash mines containing carnallite, and especially where sylvinite overlies carnallite. It is generally believed that this reversal of the normal depositional sequence may be caused by dissolution of carnallite. To obtain sylvite (KCl) from carnallite ore in the present study, first carnallite ore dissolution was performed in an aqueous solution at 25 °C, and then the sylvite was separated from halite (NaCl) in the sylvinite by a flotation method. The Br and Rb concentrations in the sylvite derived from the carnallite ore were determined. The results showed that more than 4/5th of the Br and Rb in the carnallite ore transferred to the mother liquor, while the remainder of the Br and Rb was in the sylvinite. The sylvite separated from this sylvinite had purity of 94–96%. In the sylvite derived from carnallite, the Br concentration was obviously lower (by an order of magnitude) than the concentration in primary sylvite from evaporation of $MgSO_4$-deficient sea water, and the Rb concentration was twice that in primary sylvite from evaporation of $MgSO_4$-deficient sea water. Compared to the Br and Rb concentrations in secondary sylvite from Khorat Plateau, Sergipe, and Prairie evaporites, the concentrations in the sylvite derived from carnallite ore were similar. The redistribution of Br and Rb in the form of secondary sylvite was in a relative stable proportion according to the comparison of Br and Rb. The lower Br and higher Rb concentrations in sylvite derived from carnallite ore could be caused by KCl re-crystallization and redistribution of Br and Rb between the solid and liquid phases. The driving force behind changes in the partition coefficients of Br and Rb is that the dissolution of carnallite is much slower than the nucleation of KCl.

1. Introduction

The concentrations of major and trace elements co-precipitated with evaporative minerals may be used as a geochemical indicator for the conditions during their formation. Trace elements, especially Br and Rb, are more sensitive to changes in the formation environment than major elements, and are often used as genetic and metamorphism indicator in salt deposits (Valyashko, 1956; McIntire, 1963, 1968; Kühn, 1968, 1972; Herrmann, 1980; Garrett, 1996; Warren, 1999; Taberner et al., 2000; Rahimpour-Bonab and Alijani, 2003; Siemann, 2003; Rahimpour-Bonab and Kalantarzadeh, 2005; Cheng et al., 2008). Br does not form its own minerals but substitutes for Cl ion in halite, sylvite, carnallite, and bischofite (Cheng et al., 2008). Rb does not form its own minerals during halogenesis, however, solid solutions are predominant in carnallite, and isomorphous substitutions, in sylvite (Zherebtsova and Volkova, 1966; Osichkina, 2006). A method that most investigators have employed to make the problem easier is to calculate distribution coefficients, and then use these values to estimate the Br and Rb contents of various salts in a mixture, or guess at a "theoretical" Br and Rb values for the deposit. However, such distribution coefficients are often strongly influenced by temperature, other ions and the rate of crystallization (Garrett, 1996).

The following four types of relationship between sylvite and carnallite are considered: (1) the rocks are facies equivalents deposited in different areas from essentially contemporaneous brines; (2) carnallite formed by reaction of sylvite with magnesium chloride brines; (3) sylvite derived from carnallite by leaching of magnesium chloride; (4) sylvite, as presently found, not directly related to carnallite, but formed through solution of pre-existing sylvite with subsequent crystallization (Wardlaw, 1968; Cheng et al., 2014). However, one of these relationships, in which sylvite is derived from carnallite by leaching of magnesium chloride, is considered very important for the formation of secondary sylvite (Wardlaw, 1968; Hite and Japakasetr, 1979; Cheng et al., 2014). We have investigated changes in the Br and Rb concentrations in sylvite derived from carnallite by leaching of magnesium chloride. The results suggest that low Br and high Rb concentrations in sylvite are characteristic of secondary sylvite formation from carnallite (Cheng et al., 2014).

* Corresponding author at: Qinghai, Institute of Salt Lakes, Chinese Academy of Science, Xi'ning 810008, China.
E-mail address: chenghuaide@isl.ac.cn (H.D. Cheng).

http://dx.doi.org/10.1016/j.gexplo.2016.03.016
0375-6742/

In an earlier study, a model was developed for sylvite derived from carnallite by fresh-water leaching of magnesium chloride under isothermal conditions at 25 °C where no evaporation occurs at saturation with KCl, and this gave for Br and Rb concentration ranges of 0.10–0.90 mg/g and 0.01–0.18 mg/g, respectively (Wardlaw, 1968). In another study, a model was developed for primary sylvite with normal evaporation deposits from $MgSO_4$-deficient sea water, which gave Br and Rb concentration ranges of 2.89–3.54 mg/g and 0.017–0.02 mg/g, respectively (Braitsch, 1962; Braitsch, 1966). Previous research (Cheng et al., 2014) suggests that sylvite derived from carnallite will contain less Br and more Rb than primary sylvite. This will occur because of complete dissolution of carnallite or incongruent dissolution.

The main goal of this research was to provide scientific evidence for the changes in the concentrations of the trace elements (Br, Rb) in secondary sylvite derived from carnallite ore by a simulation of carnallite dissolution in an aqueous solution at 25 °C, and to discuss the driving force behind these changes.

2. Experimental

2.1. Materials and analytical methods

A core sample of carnallite ore was obtained by drilling from a potash deposit in Vientiane, Laos. Its composition (Table 1) indicates that the core sample mainly includes carnallite and halite. The content of water-insoluble materials and sylvite in the carnallite ore were <1%, and <0.3%, respectively. The octadecyl amine (ODA; 98% pure; Dachat Chemical Inc., Zhejiang, China) as the collector was used in flotation separation experiments. Double distilled water was used in all the experiments, as well as for the analytical measurements. Standard glassware was used in all experiments. Whenever heating was required, a super constant temperature water-bath (HH-501, Shanghai Qiqian Electronic Technology Co. Ltd., China) was used. The solid phases were obtained by vacuum filter (SHZ-3 circulating water vacuum pump, Shanghai Yarong Biochemistry Factory, China) separation. Whenever agitating was required, an agitator (IKA Eurostar 200, Ningbo Scientz Biotechnology Co. Ltd., Zhejiang, China) was used. A flotation machine (XFDIII-1.0 L, Jilin Prospecting Machinery Factory, Jilin, China) was used in flotation separation experiments.

The K^+, Na^+, Mg^{2+}, Cl^-, Br^- and Rb^+ concentrations were measured at the Qinghai Institute of Salt Lakes of the Chinese Academy of Science (Qinghai, China). The analytical methods are listed in Table 2.

2.2. Experimental procedures

The decomposition of carnallite in an aqueous solution is an example of incongruent dissolution. When water contacts with the carnallite, the rhombic crystals dissolve and, because of the common ion effect, small cubic KCl crystals form in the vicinity of the dissolving carnallite (Emons and Wouny, 1981; Emons and Voigt, 1981; Xia et al., 1993; Hong et al., 1994; Liu et al., 2007). As time passes, the KCl crystals grow. To simulate secondary sylvite formation from carnalite, the carnallite ore was placed in an aqueous solution in a 2 L flask for dissolution, as detailed in an earlier study (Cheng et al., 2015). The decomposition process of carnallite in aqueous solution was an endothermic reaction, and was carried out in a super constant temperature water-bath. The reaction temperature was controlled at 25 ± 0.5 °C. The speed of the agitator was 100 rpm, and the reaction time was 90 min. The solid-phase minerals and liquid-phase solution were separated by vacuum filtration after the end of decomposition. The particle size of the carnallite ore used in our experiments was between 5 and 8 mm.

Table 2
The Analytical methods in this study.

Ions	Analytical methods	Accuracy
K^+	Gravimetric method with sodium tetraphenylborate	±0.3%
Mg^{2+}	Complexometric titration with an EDTA standard solution	±0.5%
Cl^-	$Hg(NO_3)_2$ titration	±0.5%
Br^-	Fluorescence method	±0.5%
Rb^+	Inductively coupled plasma atomic emission spectroscopy	±0.5%
Na^+	Calculated by the ion-equilibrium subtraction method	±1%

So that the Rb^+ and Br^- concentrations in halite and sylvite could be determined individually, halite and sylvite in the solid-phase minerals were separated in a single-trough flotation machine at 25 ± 0.5 °C, using ODA as the collector. To prepare 2% (mass fraction) dispersions of ODA in water, ODA was heated to 70 °C. Once the ODA had melted, it was mixed with 100 mL of distilled water containing HCl (also at 70 °C). The volume of HCl used was calculated to achieve a 1:1 M ratio of ODA to HCl. The flotation operation was carried out in two stages namely roughing and scavenging. The reagent conditioned feed puple is treated in a first stage called rougher. The tailing from the rougher stage, which may still contain some valuable mineral particles, is treated in another stage called scavenger. The scavenger tailing is the final tailing.

2.3. Data processing

There was mother liquor adsorbed to the crystals/minerals in the solid products obtained by vacuum filtration of the dissolution solution, and this affected the results. Therefore to estimate the concentrations of Br^- and Rb^+ in pure solid phases without mother liquor, the following calculation was used:

$$Br_{P-solid}(Rb_{P-solid}) \cdot X_{P-solid} + Br_L(Rb_L) \cdot X_L = Br_D(Rb_D) \cdot (X_{P-solid} + X_L) \quad (1)$$

where X_L is the mass fraction of the mother liquor solution adsorbed to the crystals/minerals in the dissolution products obtained after separation by vacuum filtration, which was calculated based on the Mg^{2+} ion concentrations in the crystals/minerals (Cheng et al., 2015); $X_{P\text{-}solid}$ is the mass fraction of the pure solid phase after removal of the mother liquor; Br_D and Rb_D are the concentrations of Br and Rb in the dissolution products obtained after separation by vacuum filtration; $Br_{P\text{-}Solid}$ and $Rb_{P\text{-}solid}$ are the concentrations of Br and Rb in the pure solid phases after removal of the mother liquor; and Br_L and Rb_L are the concentrations of Br and Rb in the mother liquor. In principle, $X_{P\text{-}solid} + X_L$ should equal 100%.

Eq. (1) can be solved for $Br_{P\text{-}solid}$ and $Rb_{P\text{-}solid}$, using Eq. (2) and Eq. (3), respectively

$$Br_{P-solid} = \frac{Br_D \cdot (X_{P-solid} + X_L) - Br_L X_L}{X_{P-solid}} = \frac{Br_D - Br_L X_L}{X_{P-solid}} \quad (2)$$

Table 1
The composition of a core sample from a potash deposit in Vientiane, Laos.

Major ion concentrations, mg/g				Substance components, wt.%				Mineral phases, wt.%			
K	Mg	Cl	Na	KCl	NaCl	$MgCl_2$	H_2O	Carnallite	Sylvite	Halite	Water-insoluble materials
83.50	51.00	469.90	159.73	15.92	40.59	19.98	23.51	58.28	0.28	40.59	0.85

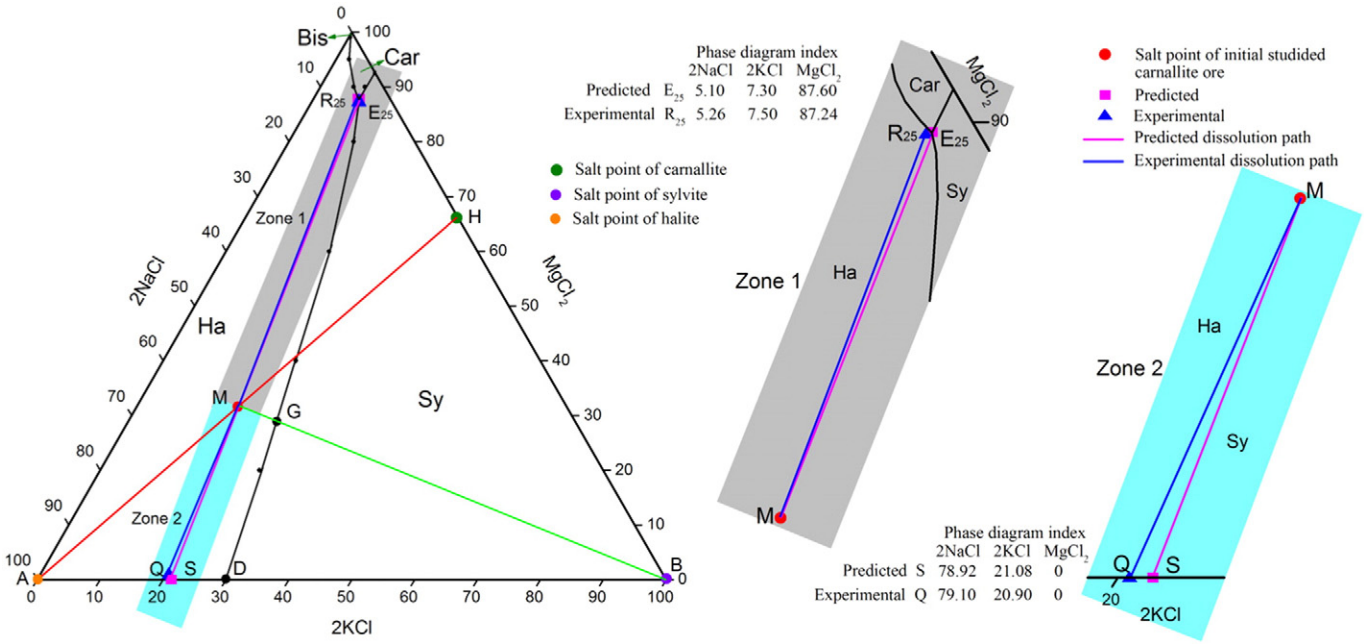

Fig. 1. Quaternary diagram of NaCl–KCl–$MgCl_2$–H_2O system at 25 °C. The compound names are abbreviated as follows: Sy = KCl, Ha = NaCl, Car = KCl·$MgCl_2$·$6H_2O$, and Bis = $MgCl_2$·$6H_2O$.

$$Rb_{P-solid} = \frac{Rb_D \cdot (X_{P-solid} + X_L) - Rb_L X_L}{X_{P-solid}} = \frac{Rb_D - Rb_L X_L}{X_{P-solid}}. \quad (3)$$

The concentrations of major elements in the pure solid phases after removal of the mother liquor can be calculated formulas as follows:

$$M_{P-solid} = \frac{M_D - M_L X_L}{X_{P-solid}} \quad (4)$$

where M represents K, Mg, Cl, or Na, M_D is the concentration of the relevant ion in dissolution products obtained after separation by vacuum filtration, and M_L is the concentration of K, Mg, Cl or Na in the mother liquor.

The mass of the products was always lower than the mass of the feed because of the viscosity of the brine and some solution adsorbed to the surface of the container in the experiments. When the mass of the solid phase in the products was weighed using electronic balance (accuracy ± 0.01 g), the loss of mass of the system was equal to the mass of the liquid phase, which could be calculated by mass balance of the feed and the products.

According to the recommendations of McIntire (1963) and Beattie et al. (1993), the partition coefficient between the solid and the liquid phases (D_{Br} or D_{Rb}) was calculated as follows:

$$D_{Br(Rb)} = \frac{\text{mass} - \%\text{Br}(Rb)_{solid-solution}}{\text{mass} - \%\text{Br}(Rb)_{aqueous-solution}}. \quad (5)$$

To compare our experimental data with that from other studies, the published values in the original papers were recalculated in mg/g.

3. Results and discussion

3.1. NaCl–KCl–$MgCl_2$–H_2O quaternary system

The quaternary system of NaCl–KCl–$MgCl_2$–H_2O is particularity important for $MgSO_4$-deficient salt deposits. It is characterized by appearance of the ternary compound carnallite (KCl·$MgCl_2$·$6H_2O$). Fig. 1 shows a projection of the 25 °C isotherm of the quaternary system (NaCl–KCl–$MgCl_2$–H_2O). The graphical representation of the quaternary system, during the carnallite ore dissolution in aqueous solution, is based on the phases diagram index (mole Σ 2NaCl + 2KCl + $MgCl_2$ = 100). In this diagram the phases diagram index are expressed as follows:

$$2\text{NaCl}\% = \frac{n[2\text{NaCl}]}{D} \times 100; 2\text{KCl}\% = \frac{n[2\text{KCl}]}{D} \times 100; \text{MgCl}_2\% = \frac{n[\text{MgCl}_2]}{D} \times 100 \quad (6)$$

where, "n" is the mole number and D = n[2NaCl] + n[2KCl] + n[$MgCl_2$].

In Fig. 1, H represents the salt point of carnallite, A represents the salt point of halite, B represents the salt point of sylvite, and E_{25} is the point at which the solution is saturated with carnallite, halite, and sylvite. In this study, the results showed that the studied carnallite ore is mainly

Table 3
The composition of solid and liquor phases after dissolution of carnallite ore at 25 °C.

Component	Weight, g experiment	Weight, g modified	Major element, mg/g				Minor element, mg/g		Substance components, wt.%			Mother liquor inclusion, wt.%
			K	Mg	Cl	Na	Rb	Br	$MgCl_2$	NaCl	KCl	
Carnallite ore	500.00	–	83.50	51.00	469.90	159.73	0.0243	1.85	19.98	40.59	15.92	–
Water	164.71	–	–	–	–	–	–	–	–	–	–	–
Sylvinite	296.85	–	119.50	7.00	533.30	262.64	0.0103	1.07	2.74	66.75	22.79	10.92
Mother liquor	366.38	400.28	17.70	64.10	213.50	7.31	0.0246	1.86	25.11	1.86	3.38	–
P–sylvinite	–	264.43	131.98	0.00	572.50	293.94	0.0085	0.97	0.00	74.71	25.17	–

composed of K^+, Na^+, Mg^{2+} and Cl^- (Table 1). The dissolution path of such kind of carnallite ore can be predicted by using the quaternary system diagram (NaCl–KCl–$MgCl_2$–H_2O) at 25 °C. The prediction of dissolution path during the dissolution of carnallite ore in aqueous solution is mainly based on the location of phases diagram index (mole Σ 2NaCl + 2KCl + $MgCl_2$ = 100) of initial studied carnallite ore on the quaternary system diagram at 25 °C. As shown in Fig. 1, M represents the salt point of initial studied carnallite ore, which lies on the stability field of halite. Moreover, M lies on line A-H. When water is added to the carnallite ore, the point for the mother liquor moves along the M-E_{25} line as the carnallite dissolves, and the point for the dissolved solid phase moves along the M-S line as sylvite crystallizes, where S is an intersection point of E_{25}-M line extension and A-B line (Zone 1 of Fig. 1). If the $MgCl_2$ content of the mother liquor is at or near the triple-saturation point E_{25}, which is the point at which the solution is saturated with carnallite, halite, and sylvite, the solubility of sylvite is suppressed to the point where most of the sylvite will precipitate, while salt point of dissolved solid phase is located at point "S" (Fig. 1). When more water is added to the system, the point for the mother liquor moves along the E_{25}-D line as sylvite dissolves, and further sylvite will disappear as the $MgCl_2$ of the solution reduces along the reaction boundary until point G is reached (Fig. 1). Accordingly, if the mother liquor will reach the "E_{25}" point, the predicted dissolution path should appear in sequences as follows:

"M": salt point of initial studied carnallite ore.

"M-E_{25}": predicted dissolution path of mother liquor.

"M-S": predicted dissolution path of dissolved solid phase.

3.2. Leaching dissolution of carnallite ore

The composition of the solid and liquid phases after dissolution of carnallite ore are given in Table 3. These results suggest the following: (1) carnallite ore (1.85 mg/g of Br, and 0.0243 mg/g of Rb) dissolved in fresh water, will produce sylvinite (0.97 mg/g of Br, and 0.085 mg/g of Rb), in which sylvinite would be defined as a mixture of sylvite and halite; and (2) 80.48% of the Br and 81.04% of the Rb in the carnallite ore will dissolve into the mother liquor, with some of this incorporated into the sylvinite product. The phases diagram index of 2NaCl, 2KCl and $MgCl_2$ of the solid and liquid phases after dissolution of the carnallite ore in the lab were calculated from the data given in Table 3 and shown in Table 4. The following are obvious from Fig. 1 and Table 4: (1) the system point M for the carnallite ore in our work lies on the lines from halite to carnallite, as illustrated by AH; (2) the system point R_{25} for the mother liquor in our experiments is similar to point E_{25} for the triple-saturation point in the NaCl–KCl–$MgCl_2$–H_2O quaternary system (Zone 1 of Fig. 1); and (3) the system point Q for the terminal product sylvinite is close to point S for the predicted salt point (Zone 2 of Fig. 1). The real dissolution path should appear as follows:

"M": salt point of initial studied carnallite ore.

"M-R_{25}": experimental dissolution path of mother liquor.

"M-Q": experimental dissolution path of dissolved solid phase.

These results indicate that: (1) the experimental dissolution path shows good agreement with the predicted dissolution path; (2) the dissolution process of carnallite ore in aqueous solution at 25 °C in this paper corresponds well with the earlier well-established model (Cheng et al., 2015).

3.3. Separation of sylvite and halite from sylvinite

Sylvite and halite are commonly separated by flotation with amine as a collector (Miller et al., 1992, 1997; Miller and Yalamanchili, 1994; Yalamanchili et al., 1993; Titkov, 2004; Burdukova et al., 2009; Laskowski, 2013). In our work, we first performed a rough separation, and then further separation of any remaining in the solution. The results of the separation experiment are presented in Table 5. The concentrations of Na^+, K^+, Mg^{2+}, Cl^-, Br^- and Rb^+ in P-solid phases products without mother liquor were calculated from the data given in Table 5 by Eqs. (1)–(4), and are shown in Table 6. As shown in Table 6, the P-solid phase products involving P-sylvinite, P-rougher concentrate, P-scavenger concentrate and P-tailing are mainly composed of halite and sylvite, and can be considered as sylvinite. We found that: (1) the P-rougher concentrate from the initial separation contained 0.37 mg/g Br and 0.0505 mg/g Rb, and sylvite (KCl) was >96% pure; (2) the P-scavenger concentrate from the second separation contained 0.42 mg/g Br and 0.0480 mg/g Rb, and sylvite (KCl) was >94% pure; and (3) the P-tailing contained 1.25 mg/g Br and −0.0015 mg/g Rb, and halite (NaCl) was >98% pure. As the KCl content decreased, the Br concentration increased and the Rb concentration decreased. The negative concentration of Rb in P-tailing occurred because the Rb concentration in the flotation tailing was not determined.

Table 4
Phase diagram index of solid and liquor phases for predicted and experimental results at 25 °C.

Component	Phases diagram index			System point
	2NaCl	2KCl	$MgCl_2$	
Carnallite ore	52.30	16.08	31.61	M
Carnallite	–	33.33	66.67	H
Sylvinite-experimental	79.10	20.90	–	Q
Sylvinite-predicted	78.92	21.08	–	S
Mother liquor-experimental	5.26	7.50	87.24	R_{25}
Triple-saturation point-predicted	5.10	7.30	87.60	E_{25}

3.4. Contents variation of Br and Rb in sylvite derived from carnallite ore

Although the sylvite derived from carnallite ore was separated from halite by a flotation method, the obtained halite and sylvite were not 100% pure. Fig. 2 shows the relationship between Br concentration and compositions of different types of P-solid phase products involving P-sylvinite, P-rougher concentrate, P-scavenger concentrate and P-tailing (Table 6). The NaCl content was positively correlated to the Br concentration, with a correlation coefficient of 0.9949. The KCl content was inversely proportional to the Br concentration, with a correlation coefficient of 0.9932. The average concentrations of Br in halite (100% NaCl) and sylvite (100% KCl) derived from carnallite ore were calculated at 1.24 and 0.35 mg/g, respectively, by linear extrapolation (Fig. 2). Fig. 3 shows the relationship between the Rb concentration and the compositions of different types of P-solid phase products involving P-sylvinite, P-rougher concentrate, P-scavenger concentrate and P-tailing (Table 6). The results indicated that: (1) the NaCl content was inversely proportional to the Rb concentration, with a correlation coefficient of 0.9974; (2) the KCl content was positively correlated to the Rb concentration, with a correlation coefficient of 0.9976 (Fig. 3). The average Rb concentrations in halite (100% NaCl) and sylvite (100% KCl) derived from carnallite were calculated at −0.0039 and 0.0515 mg/g, respectively, by linear extrapolation (Fig. 3). The similar reason for the negative concentration of Rb in halite is that the Rb concentration in the flotation tailings was not determined.

3.5. Contents variation of Br, Rb in primary and secondary sylvite from $MgSO_4$-deficient marine evaporites

The concentrations of Br, Rb in primary and secondary sylvite from Khorat Plateau, Sergipe and Prairie evaporites are listed in Table 7, and are shown in Fig. 4 and Fig. 5.

The Khorat Plateau in northeastern Thailand and central Laos is a part of the Indochina terrane and is divided into the Khorat Basin to the south and the Sakon Nakon Basin to the north by the Phu Pan Anticline. Potash deposits in the Khorat Plateau are in the Cretaceous Maha Sarakham Formation. Some authors insist that the Maha Sarakham Formation is not of marine origin (Utha-Aroon, 1993; Garrett, 1996; Warren, 1999; Meesook, 2000; Racey and Goodall, 2009). However,

Table 5
The results of an experiment separating sylvite and halite from sylvinite at 25 °C.

Component	Weight, g experiment	Major element, mg/g				Trace element, mg/g		Substance components, wt.%			Mother liquid inclusion, wt.%
		K	Mg	Cl	Na	Rb	Br	NaCl	KCl	$MgCl_2$	
Sylvinite	715.00	119.50	7.00	533.30	262.64	0.0103	1.07	66.75	22.79	2.74	10.92
Rough concentrate	160.36	434.33	9.19	437.22	10.91	0.0468	0.58	2.77	82.82	3.60	14.34
Scavenger concentrate	11.76	459.03	5.11	463.7	21.26	0.0461	0.53	5.41	87.52	2.00	7.97
Tailing	515.20	12.62	3.62	586.7	366.71	–	1.28	93.21	2.41	1.42	5.65

Table 6
The concentrations of Na^+, K^+, Mg^{2+}, Cl^-, Br^- and Rb^+ in P-solid phases products without mother liquor during the experimental separation at 25 °C.

Component	Weight, g m odified	Major element, mg/g				Trace element, mg/g		Substance components, wt.%		
		K	Mg	Cl	Na	Rb	Br	NaCl	KCl	$MgCl_2$
P-synivite	636.92	131.98	-	572.50	293.94	0.0085	0.97	74.71	25.17	-
P-rough concentrate	137.36	504.06	-	474.66	11.51	0.0505	0.37	2.67	96.37	-
P-scavenger concentrate	10.82	497.26	-	485.37	22.47	0.0480	0.42	5.72	94.82	-
P-tailing	486.09	12.32	-	609.04	388.23	−0.0015	1.25	98.65	2.34	-

evidences from Br content in halite (Hite and Japakasetr, 1979), sulfur isotopes from anhydrites (El Tabakh et al., 1999), boron isotope composition in fluid inclusion of halite (Tan et al., 2010), and boron isotope composition in borate in the potash layer (Zhang et al., 2013) showed that the evaporites in Khorat Plateau are marine deposits. Primary and secondary sylvite from potash deposits in the Khorat Plateau have been analyzed (Qu, 1980; Hite and Japakasetr, 1979; Zhang et al., 2015). These studies found a Br concentration of 2.4 mg/g in brownish primary sylvite from one core sample (K48, Wanorn Niwat in the Sakon Nakhon Basin), which was very similar to the concentration range in the model for primary sylvite (Fig. 4). In addition, the average concentration of Br in secondary sylvite from the Khorat Plateau was 0.45 mg/g, the Br concentration range in secondary sylvite from one core sample (ZK309, Savannakhet Basin) was 1.349–1.693 mg/g and the Br concentration range in milky secondary sylvite from one core sample(K49, Khon Kaen in the Khorat Basin) was 0.2–0.3 mg/g. These Br concentrations are too low for the deposit to be considered a primary sylvite, but they are close to concentrations given by the model for sylvite derived from carnallite (Fig. 4).

From the regional petrology and the lower than expected Br levels in sylvite in the Prairie Evaporite Formation (Saskatchewan, Canada), researchers have postulated a series re-crystallization events form the sylvite as a result of periodic flushing by hyper-saline solutions (Schwerdtner, 1964; Wardlaw and Watson, 1966; Wardlaw, 1968).

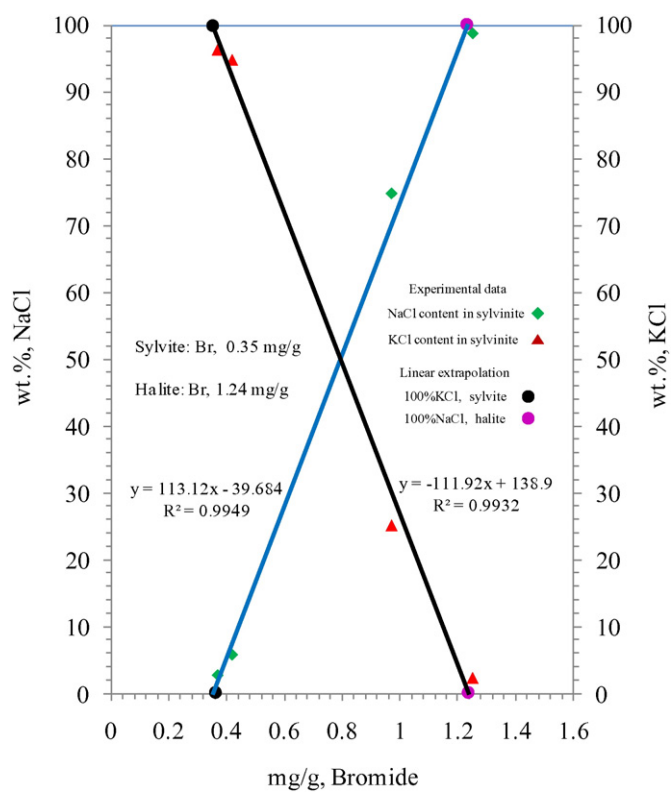

Fig. 2. Relationships between the concentration of Br and the NaCl, KCl contents in sylvinite.

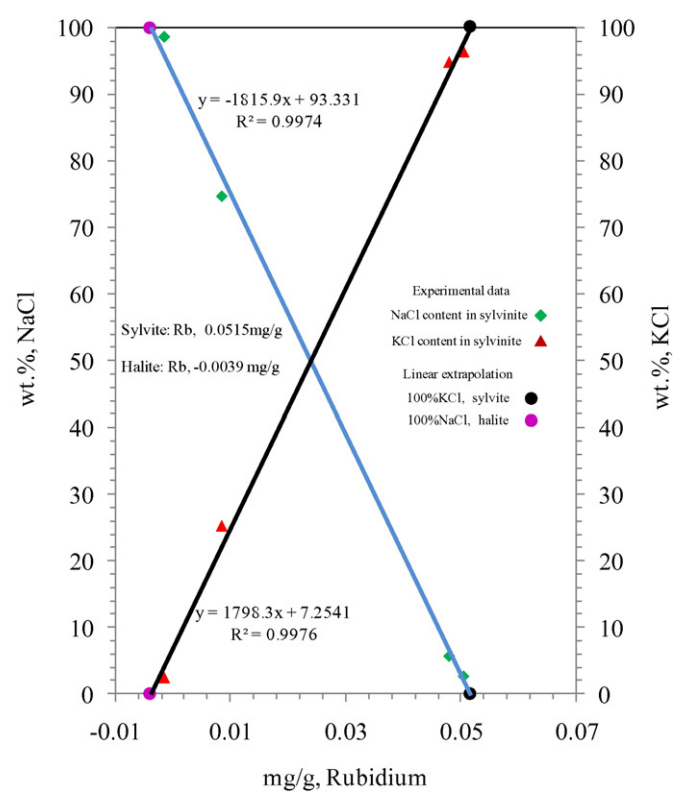

Fig. 3. Relationships between the concentration of Rb and the NaCl, KCl contents in sylvinite.

Table 7
The concentrations of Br, Rb in primary and secondary sylvite from Khorat Plateau, Sergipe deposits and Prairie evaporites.

	Primary sylvite, mg/g		Secondary sylvite, mg/g		References
	Br	Rb	Br	Rb	
Khorat Plateau	–	–	0.45	0.035	Hite and Japakasetr, 1979
	2.4	–	–	–	Qu, 1980
	–	–	0.2–0.3	–	Qu, 1980
	–	–	1.349–1.693	0.027–0.040	Zhang et al., 2015
Sergipe deposits	–	–	0.83–1.34	0.018–0.055	Wardlaw, 1972
Prairie evaporites	–	–	0.427–1.533	0.007–0.097	Wardlaw, 1970
	–	–	0.597–1.919	–	Schwerdtner and Wardlaw, 1963; Schwerdtner, 1964
	1–3.03	0–0.03	0.1–2.6	0.01–0.2	Wardlaw, 1968
Vientiane potash	–	–	0.35	0.0515	In this study
Model for primary sylvite	2.89–3.54	0.017–0.02	–	–	Braitsch, 1962, 1966
Model for secondary sylvite	–	–	0.10–0.9	0.018–0.18	Wardlaw, 1968

This classification as a secondary precipitate is supported by observations of intergrowth and overgrowth textures (McIntosh and Wardlaw, 1968), large-scale collapse and dissolution features (Gendzwill, 1978), radiometric ages (Baadsgaard, 1987), fluid inclusion evidence (Chipley and Kyser, 1989) and paleomagnetic orientations of the diagenetic hematite linings associated with the emplacement of the potash (Koehler et al., 1997). The distribution of traces of Br and Rb in the chloride minerals indicates that red sylvinite was formed by dissolution of carnallite, where red sylvite has replaced carnallite and inherited iron-oxide inclusion from carnallite (Wardlaw, 1968). Comparison of the Br and Rb concentrations in primary and secondary sylvite from the Prairie Evaporite (Schwerdtner and Wardlaw, 1963, Schwerdtner, 1964; Wardlaw, 1968, 1970) with the models for primary sylvite and sylvite derived from carnallite showed the following: (1) the range for the Br concentration clear sylvite from the Prairie Evaporite (1.00–3.03 mg/g) is very similar to that for the model for primary sylvite; (2) the range for the Br concentration in red sylvite from the Prairie Evaporite (0.1–2.6 mg/g) is close to that for the model of sylvite derived from carnallite; (3) the range for the Rb concentration in clear sylvite from the Prairie Evaporite (0–0.03 mg/g) is very close to that for the model for primary sylvite; (4) the range for the Rb concentration in red sylvite from the Prairie Evaporite (0.01 to 0.20 mg/g) is very close to that for the model for sylvite derived from carnallite, but is far in excess of that for the model for primary sylvite (Fig. 4 and Fig. 5).

Br^- measurements from halites of the Ibura Member Evaporite from Sergipe salts have values up to 0.2 mg/g in the halite–anhydrite facies (Szatmari et al., 1979). These values of Br^- in halite are similar to those in other marine evaporites (Holser, 1979), which suggests the Ibura Member salts formed from Cretaceous seawater (Timofeeff et al., 2006). In contrast to halite and carnallite from Sergipe, sylvites show Br^- concentrations less than half the values that would be expected for a primary marine deposit, which suggests that the sylvite is a secondary deposit. Similarity, there is more Rb in Ibura sylvite than in primary sylvite from present-day seawater, but the Rb concentration in carnallite is within the primary range. Therefore, Rb and Br concentrations in Sergipe carnallite are both within the ranges of a primary deposit from seawater, but Sergipe sylvite has abnormally low Br concentrations and abnormally high Rb concentrations. These relationships can be explained satisfactorily if the sylvite is formed by a secondary leaching products from carnallite (Wardlaw, 1972). Comparison of the Br and Rb concentrations in secondary sylvite from the Prairie Evaporite (Wardlaw, 1972) with the concentration ranges from the models for primary sylvite and sylvite derived from carnallite showed the following: (1) the Br concentration range in secondary sylvite from the Sergipe Evaporite (0.83–1.34 mg/g) was lower than that from the model for primary sylvite, but was close to that from the model for sylvite derived from carnallite; (2) the Br concentrations in secondary sylvite from the Sergipe evaporites was higher than those in secondary sylvite from the Khorat Plateau and Prairie evaporites, which could be caused by high Br concentration in primary carnallite from the Sergipe evaporite; and (3) the Rb concentration range in secondary sylvite from the Sergipe evaporites (0.018–0.055 mg/g) was very close to that for the model for sylvite derived from carnallite, but was much higher than that for the model for primary sylvite (Fig. 4 and Fig. 5).

In our work, the carnallite ore from potash deposits in Vientiane, Laos gave 1.85 mg/g Br and 0.0243 mg/g Rb when dissolved in fresh water. This would result in sylvite with 0.35 mg/g Br and 0.0515 mg/g Rb. As shown in Fig. 4 and Fig. 5, these concentrations are close to

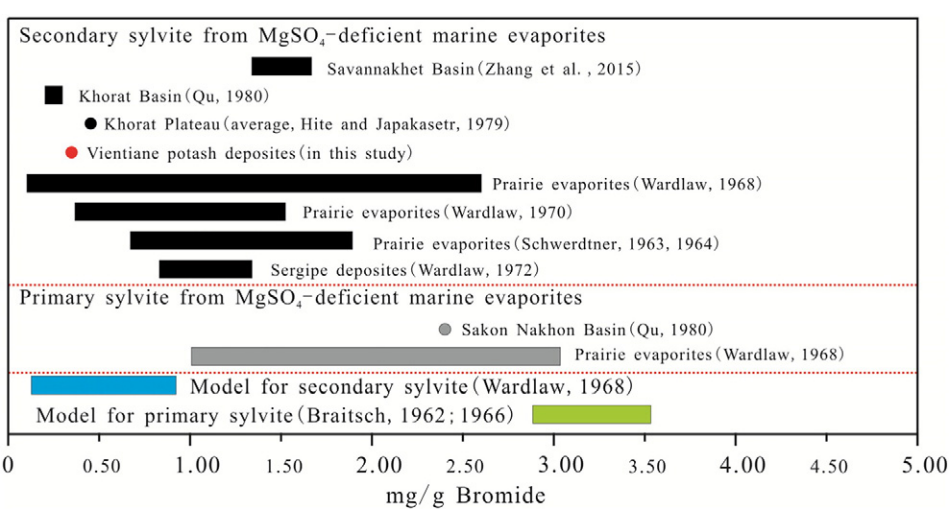

Fig. 4. Br values of primary and secondary sylvite from $MgSO_4$-deficient evaporites.

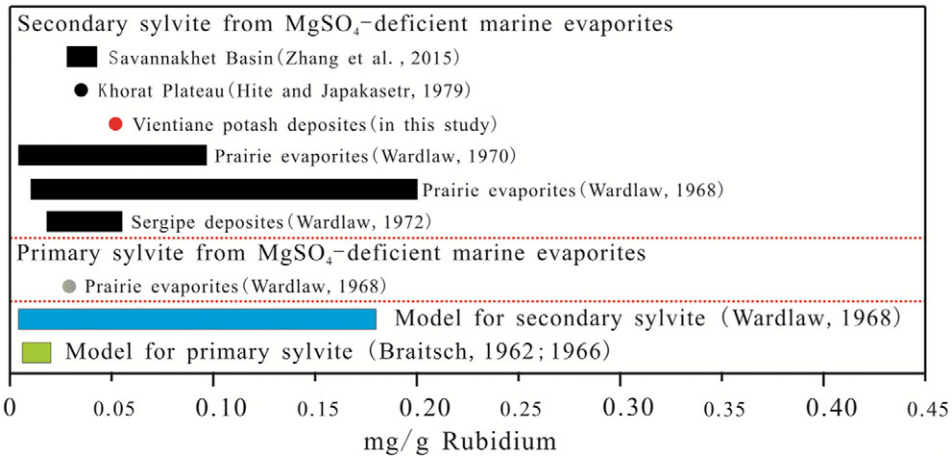

Fig. 5. Rb values of primary and secondary sylvite from $MgSO_4$-deficient evaporites.

those in secondary sylvite from the Khorat Plateau, Sergipe and Prairie evaporites, close to the concentrations for the model for sylvite derived from carnallite (Wardlaw, 1968), and lower than the Br concentration and higher the Rb concentration for the model for primary sylvite (Braitsch, 1962; Braitsch, 1966).

3.6. Comparison with Br and Rb values of secondary sylvite from $MgSO_4$-deficient marine evaporites

Previous researches on the origin of secondary sylvite from $MgSO_4$-deficient marine evaporites (Khorat Plateau, Sergipe and Prairie evaporites) indicated that Br and Rb values of secondary sylvite have an obvious changes compared with primary sylvite, and concluded that secondary sylvite contains less Br and more Rb than primary sylvite (Wardlaw, 1968; Hite and Japakasetr, 1979; Qu, 1980; Cheng et al., 2014; Zhang et al., 2015). This phenomenon was explained that the secondary sylvite derive from carnallite by leaching of magnesium chloride. We compared Br and Rb values of a model (Wardlaw, 1968) for secondary sylvite, and found that Br have strong correlation (R^2 = 0.9804) with Rb (Fig. 6). The comparisons between Br and Rb in secondary sylvite from the Khorat Plateau, Sergipe and Prairie evaporites indicated that the varying trend of those values is similar to a model for secondary sylvite (Fig. 6). According to the comparison of Br and Rb, the redistribution of Br and Rb in the form of secondary sylvite was in a relative stable proportion. The comparison seems to verify our inference that secondary sylvite derive from carnallite by leaching of magnesium chloride. This result is consistent with the observation from our experiment on leaching dissolution of carnallite ore from potash deposit

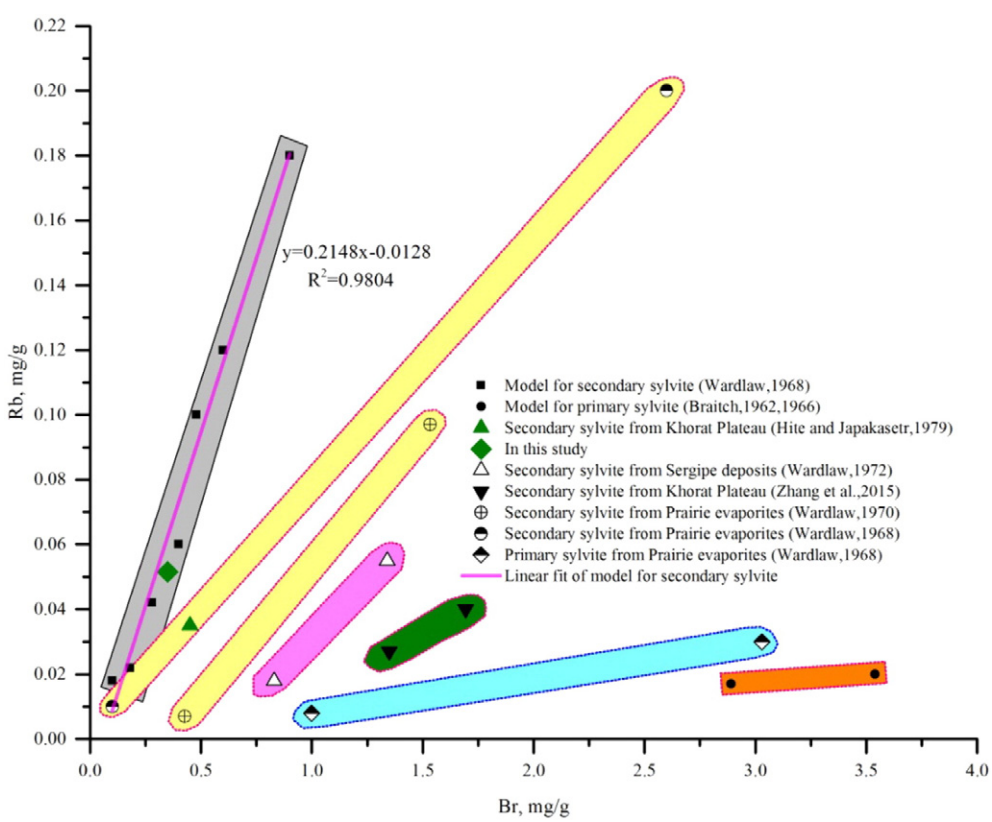

Fig. 6. Relationships between Br and Rb values of secondary sylvite from $MgSO_4$-deficient evaporites.

Table 8
The values of D_{Br} in sylvite produced by evaporation in various systems at 25 °C.

Systems	D_{Br}	Br concentrations in mother liquor, mg/g	References
K//Cl, Br–H_2O	0.81 ± 0.05	0.026–9.76	Braitsch and Herrmann, 1964
K, Na//Cl, Br–H_2O	0.80 ± 0.05	1.09–5.56	Braitsch and Herrmann, 1964
K, Na, Mg//Cl, Br–H_2O	0.73 ± 0.04	1.21–7.54	Braitsch and Herrmann, 1964
K, Ca, Mg//Cl, Br–H_2O	0.75 ± 0.04	2.21–6.47	Braitsch and Herrmann, 1964
K//Cl, Br–H_2O	0.690 ± 0.014	0.024–9.209	Siemann and Schramm, 2002

in Vientiane, Laos (Fig. 6). In addition, a comparation between Br and Rb in primary sylvite from Prairie evaporites indicate that the trend of those values is similar to a model for primary sylvite (Fig. 6).

In generally, marine evaporites like those from the Khorat Plateau, Sergipe and Prairie evaporites all contain the same potassium mineral, carnallite. Production of secondary sylvite from this carnallite will occur easily because of the plasticity and solubility of saline minerals.

3.7. Partition coefficient of Br and Rb in sylvite derived from carnallite

Knowledge of the abundance and the partitioning of Br between chloride minerals and hypersaline brines is of great importance in understanding marine evaporites. Many authors have investigated the incorporation of Br in sylvite in various systems under laboratory conditions at 25 °C (Table 8). The mean of the partition coefficient of Br in sylvite in these investigations was between 0.7 and 0.8, and the distribution of Br between solid and liquid depended mainly on the composition of the aqueous solution. In the present work, carnallite ore was dissolved in fresh water, which produced sylvite containing 0.35 mg/g Br and mother liquor containing 1.86 mg/g Br. The partition coefficient of Br in sylvite derived from carnallite ore, which was calculated using Eq. (5), was 0.1886. This result shows that the partition coefficient of Br is highly sensitive to the Br content in the sylvite and the Br content in the brine. In addition, the Br content in the sylvite was lower than that in primary sylvite because the partition coefficient of Br between solid and liquid phases changes. Therefore, it should not be treated as constant for systems undergoing rapid evaporation, such as seawater in the region of sylvite and carnallite precipitation.

The equilibrium coefficient of co-crystallization of trace Rb with potassium salts was determined repeatedly. The range for the partition coefficient of Rb for sylvite was 0.113–0.652 at 0 °C, 0.10–0.21 ± 0.01 at 25 °C, and 0.09–0.984 ± 0.001 at 40 °C. At 30, 50, and 80 °C the partition coefficients were 0.94, 0.103, and 0.119, respectively (Ladynina and Anoshin, 1962; McIntire, 1968; Shock and Puchelt, 1971; Kühn, 1972; Valyashko and Petrova, 1973; Melikhov et al., 1974; Osichkina, 2006). In the present study, dissolving carnallite in fresh water produced sylvite containing 0.0516 mg/g Rb and mother liquor containing 0.0246 mg/g Rb. The partition coefficient of Rb in this sylvite, which was calculated by Eq. (5), was 2.0976. The results showed that the distribution of Rb between solid and liquid phases depended mainly on the temperature, while the value of D_{Rb} decreased as the temperature increased. In addition, the Rb concentration in secondary sylvite was much greater than that in primary sylvite because the partition coefficient of Rb between solid and liquid phases changed. Finally, the value of D_{Rb} in sylvite derived from carnallite increased because to KCl recrystallization during the dissolution process.

3.8. Driving force

The discussion in Section 3.6 and 3.7 indicates that the partition coefficients of Br and Rb in sylvite derived from carnallite can show large variations because of the incongruent dissolution of carnallite in fresh water. For dissolution of carnallite in an appropriate volume of water, $MgCl_2$ dissolves while KCl crystallizes. This process can result in KCl re-crystallization and redistribution of Br and Rb between the solid and liquid phases.

Xia et al. (1993) and Hong et al. (1994) investigated the dissolution of carnallite in pure water, and aqueous solutions of KCl and $MgCl_2$. They found the following: (1) the dissolution of K^+, Mg^{2+}, and Cl^- ions in carnallite occurred simultaneously; (2) K^+ and Cl^- in the aqueous solution from dissolution of carnallite formed KCl crystals; (3) the coupling of a high dissolution rate of carnallite and a high nucleation rate of KCl near the surface of the carnallite resulted in the formation of KCl crystals; and (4) the crystal growth of KCl from dissolution of carnallite in pure water was mainly dominated by a two-dimensional nucleation growth mechanism. Based on these results, we compared the Mg^{2+} dissolution rates and K^+ crystallization rates in three solutions, and found that the K^+ crystallization rate was higher than the Mg^{2+} dissolution rate (Fig. 7). These indicated that the low Br and high Rb concentrations in sylvite derived from carnallite were caused by changes in the trace elements' partition coefficients because the dissolution of carnallite was much slower than nucleation of KCl.

In addition, the crystal structure of carnallite consists of a network of face-sharing KCl_6 octahedra and isolated $Mg(H_2O)_6$ octahedra occupying the openings in the KCl network, with water molecules acting as charge transmitters between Mg^{2+} and Cl^- ions (Weck et al., 2014).

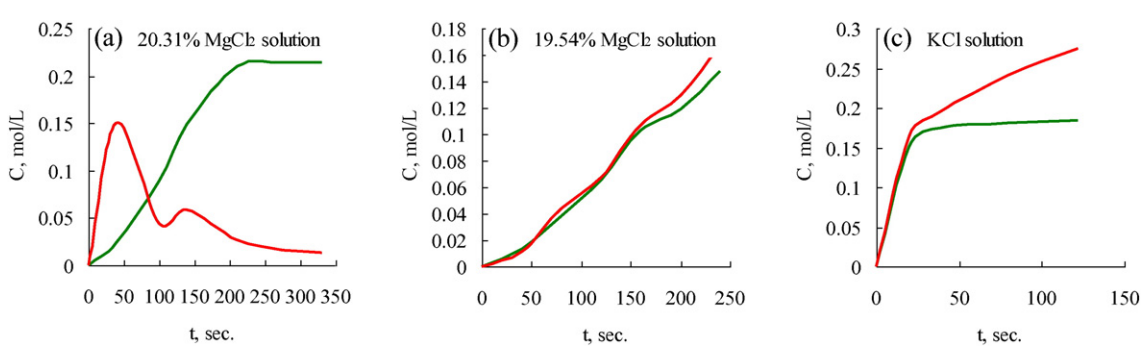

Fig. 7. Comparison of C_{Mg2+} dissolution and C_{K+} crystallization with time the following solutions during dissolution of carnallite: (a) 20.31% $MgCl_2$ solution; (b) 19.54% $MgCl_2$ solution; and (c) KCl solution. C_{Mg2+} dissolution is shown by the green solid line, and C_{K+} crystallization is shown by the red solid line. C_{Mg2+} and C_{K+} represent the concentrations of the relevant ion in solution, respectively.

Magnesium ions exist in the aqueous solution as $[Mg(H_2O)_6]^{2+}$ (Podder et al., 2013), and this promotes the $Mg(H_2O)_6$ octahedra in the carnallite to enter the solution and increases dissolution of carnallite. The solubility of KCl is low in a concentrated $MgCl_2$ solution, and a very high $MgCl_2$ concentration will be suitable for the formation of sylvite. The structure unit of $Mg(H_2O)_6$ or $[Mg(H_2O)_6]^{2+}$ may be an another factor that results in variation of the trace elements' partition coefficients.

4. Conclusions

The levels of the trace elements Br and Rb can vary in primary and secondary sylvite in evaporites, and especially in sylvite derived from carnallite by leaching of magnesium chloride. The reason for this variation is that KCl can re-crystallize and redistribution of the trace elements between the solid and liquid phases can occur during this process. In the present study, the dissolution of carnallite and formation of sylvite were studied. The results showed the following: (1) low Br and high Rb concentrations occurred in sylvite derived from carnallite; (2) the concentrations of Br and Rb in sylvite derived from carnallite were similar to those in secondary sylvite from Khorat Plateau, Sergipe, and Prairie evaporites; (3) the redistribution of Br and Rb in the form of secondary sylvite was in a relative stable proportion according to the comparison of Br and Rb (Fig. 7); and (4) the driving force behind changes in the trace elements' partition coefficients was the slower dissolution of carnallite compared with nucleation of KCl.

Acknowledgments

We specially thank two anonymous reviewers for their helpful comments. This research was supported by the West Light Foundation of CAS (2011-180) and the National Program on Key Basic Research Project of China (973 Program, Grant No. 2011CB403004).

References

Baadsgaard, H., 1987. Rb–Sr and K–Ca isotope systematics in minerals from potassium horizons in the Prairie Evaporite Formation, Saskatchewan, Canada. Chem. Geol. 66, 1–15.
Beattie, P., Drake, M., Jones, J., Leeman, W., Longhi, J., McKay, G., Nielsen, R., Palme, H., Shaw, D., Takahashi, E., Wastson, B., 1993. Terminology for trace-element-partitioning. Geochim. Cosmochim. Acta 57, 1605–1606.
Braitsch, O., 1962. Entstehung und stoffbestand der salzlagerstätten, mineralogie und petrographie in einzeldarstellungen. Springer-Verlag, Berlin.
Braitsch, O., 1966. Bromine and rubidium as indicators of environment during sylvite and carnallite deposition of the upper Rhine Valley evaporites. Second Symposium on Salt 1. The Northern Ohio geological society, pp. 293–301.
Braitsch, O., Herrmann, A.G., 1964. Zur Geochemie des Broms in salinaren Teil II:Die Bildungstemperaturen primrer Sylvin- und Carnallit-Gesteine. Geochim. Cosmochim. Acta 28, 1081–1109.
Burdukova, E., Laskowski, J.S., Forbes, G.R., 2009. Precipitation of dodecyl amine in KCl–NaCl saturated brine and attachment of amine particles to KCl and NaCl surfaces. Int. J. Miner. Process. 93, 34–40.
Cheng, H.D., Ma, H.Z., Tan, H.B., Xu, J.X., Zhang, X.Y., 2008. Geochemical characteristics of bromine in potassium deposits: review and research perspectives. Bull. Mineral. Petrol. Geochem. 27 (4), 399–408 (in Chinese with English abstract).
Cheng, H.D., Hai, Q.Y., Zhang, X.Y., Fan, Q.S., Ma, H.Z., 2014. Content variations of rubidium and bromide in sylvite derived from carnallite by leaching of magnesium chloride. Acta Geol. Sin. 88, 298–300.
Cheng, H.D., Ma, H.Z., Hai, Q.Y., Zhang, Z.H., Xu, L.M., Ran, G.F., 2015. Model for the decomposition of carnallite in aqueous solution. Int. J. Miner. Process. 139, 36–42.
Chipley, D.B.L., Kyser, T.K., 1989. Fluid inclusion evidence for the deposition and diagenesis of the Patience Lake Member of the Devonian Prairie Evaporite Formation, Saskatchewan, Canada. Sediment. Geol. 64, 287–295.
Emons, H., Voigt, H., 1981. Untersvchungen zur kalten zersetzunung von Carnallit. Freiberg Forschungsher A628, 69–78.
Emons, H., Wouny, F.W., 1981. Untersvchungen zur gezielten Beeinflussung der Korngrobe des zersetzungs-KCl bei kalten zersetzung von Carnallit. Freiberg Forschungsher A654, 117–119.
Garrett, D.E., 1996. Potash: Deposits, Processing, Properties and Uses. Springer, Berlin, pp. 1–80.
Gendzwill, D.J., 1978. Winnipegosis mounds and Prairie Evaporite Formation of Saskatchewan — seismic study. Bull. Am. Assoc. Pet. Geol. 62, 73–86.
Herrmann, A.G., 1980. Methodical investigations on the origin of brines in salt and potash mines. Fifth Symposium on Salt vol. 1. The Northern Ohio geological society, pp. 91–96.
Hite, R.J., Japakasetr, T., 1979. Potash deposits of the Khorat Plateau, Thailand and Laos. Econ. Geol. 74, 448–458.
Holser, W.T., 1979. Trace elements and isotopes in evaporites. In: Burns, R.G. (Ed.), Marine Minerals. Mineralogical Society of America Reviews in Mineralogy 6. Mineralogical Society of America, pp. 295–346.
Hong, X.L., Xia, S.P., Gao, S.Y., 1994. Dissolution kinetics of carnallite. Chin. J. Appl. Chem. 11 (3), 26–31 (in Chinese with English abstract).
Koehler, G., Kyser, T.K., Enkin, R., Irving, E., 1997. Paleomagnetic and isotopic evidence for the diagenesis and alteration of evaporites in the Paleozoic Elk Point Basin, Saskatchewan, Canada. Can. J. Earth Sci. 34, 1619–1629.
Kühn, R., 1968. Geochemistry of the German potash deposits. Geol. Soc. Am. Spec. Pap. 88, 427–504.
Kühn, R., 1972. Combined Evaluation of Br- and Rb-contents for the Genetic Characterization of Carnallites and Sylvite Rocks. Unesco, Geology of Saline Deposits. pp. 77–89.
Ladynina, I.N., Anoshin, G.N., 1962. Rubidium, thallium, and bromine partitioning during formation of potassium salt deposits. Geol. Geofiz. 3, 64–67.
Laskowski, J.S., 2013. From amine molecules adsorption to amine precipitate transport by bubbles: a potash ore flotation mechanism. Miner. Eng. 45, 170–179.
Liu, C., Ji, Y., Bai, Y., Cheng, F., Lu, X., 2007. Formation of porous crystals by coupling of dissolution and nucleation process in fractional crystallization. Fluid Phase Equilib. 261 (1), 300–305.
McIntire, W.L., 1963. Trace element partition coefficients—a review of theory and applications to geology. Geochim. Cosmochim. Acta 27 (12), 1209–1264.
McIntire, W.L., 1968. Effect of temperature on the partition of rubidium between sylvite crystals and aqueous solutions. Geol. Soc. Am. Spec. Pap. 88, 505–524.
McIntosh, R.A., Wardlaw, N.C., 1968. Barren halite bodies in the sylvinite mining zone at Esterhazy, Saskatchewan. Can. J. Earth Sci. 5, 1221–1238.
Meesook, A., 2000. Cretaceous environments of northeastern Thailand. In: Okada, H., Mateer, N.J. (Eds.), Cretaceous Environments of Asia. Elsevier, Amsterdam, pp. 207–223.
Melikhov, I.V., Berdonosova, D.G., Pakhomov, L.P., 1974. The effect of crystal collisions in mixed suspension on rubidium migration from solution to KCl crystals. Radiokhimiya 16 (3), 297–300.
Miller, J.D., Yalamanchili, M.R., 1994. Fundamental aspects of soluble salt flotation. Miner. Eng. 7, 305–317.
Miller, J.D., Kellar, J.J., Yalamanchili, M.R., 1992. Surface charge of alkali halide particals as determined by laser-Doppler electrophoresis. Langmuir 8 (5), 1464–1469.
Miller, J.D., Veeramasuneni, S., Yalamanchili, M.R., 1997. Recent contributions to the analysis of soluble salt flotation system. Int. J. Miner. Process. 51, 111–123.
Osichkina, R.G., 2006. Regularities of trace element distribution in water–salt systems as indicators of the genesis of potassium Salt rocks: an example from the upper Jurassic halogen formation of Central Asia. Geochem. Int. 44 (2), 164–174.
Podder, J., Gao, S., Evitts, R.W., Besant, R.W., Matthews, D., 2013. Synthesis of carnallite crystal from KCl-$MgCl_2$ solutions and its characterization. Int. J. Mater. Res. 104, 1–6.
Qu, Y.H., 1980. Study on sedimentation nature and genesis of potash deposits in Ale basin, Thailand. Geology of Chemical Minerals 2 (1), 13–22 (in Chinese with English abstract).
Racey, A., Goodall, J.G.S., 2009. Palynology and stratigraphy of the Mesozoic Khorat Group of NE Thailand. In: Buffetaut, E., Cuny, G., Le Loeuff, J., Suteethorn, V. (Eds.), Late Palaeozoic and Mesozoic Ecosystems in SE Asia 315. Geological Society and Special Publications, London, pp. 67–81.
Rahimpour-Bonab, H., Alijani, N., 2003. Petrography, diagenesis and depositional model for potash deposits of the Central Iran-Garmsar area and use of bromine geochemistry as a prospecting tool. Carbonates Evaporites 18, 19–28.
Rahimpour-Bonab, H., Kalantarzadeh, Z., 2005. Origin of secondary potash deposits: a case from Miocene evaporites of NW Central Iran. J. Asian Earth Sci. 25, 157–166.
Schwerdtner, W.M., 1964. Genesis of potash rocks in Middle Devonian Prairie Evaporite Formation of Saskatchewan. Bull. Am. Assoc. Pet. Geol. 48, 1108–1115.
Schwerdtner, W.M., Wardlaw, N.C., 1963. Geochemistry of bromine in some salts rocks of the Prarie Evaporite Formation of Saskatchewan. First Symposium on Salt. The Northern Ohio geological society, pp. 240–246.
Shock, H.H., Puchelt, H., 1971. Rubidium distribution in salt minerals: experimental investigations. Geochim. Cosmochim. Acta 35, 307–311.
Siemann, M.G., 2003. Extensive and rapid changes in seawater chemistry during the Phanerozoic: evidence from Br contents in basal halite. Terra Nova 15, 243–248.
Siemann, M.G., Schramm, M., 2002. Henry's and non-Henry's law behavior of Br in simple marine systems. Geochim. Cosmochim. Acta 66 (8), 1387–1399.
Szatmari, P., Carvalho, R.S., Simôes, I.A., 1979. A comparison of evaporite facies in the Late Paleozoic Amazon and the Middle Cretaceous south Atlantic salt basins. Econ. Geol. 74, 432–447.
El Tabakh, M., Utha-Aroon, C., Schreiber, B.C., 1999. Sedimentology of the Cretaceous Maha Sarakham evaporites in the Khorat Plateau of northeastern Thailand. Sediment. Geol. 123, 31–62.
Taberner, C., Cendón, D.I., Pueyo, J.J., Ayora, C., 2000. The use of environmental markers to distinguish marine vs. continental deposition and to quantify the significance of recycling in evaporite basins. Sediment. Geol. 137, 213–240.
Tan, H.B., Ma, H.Z., Li, B.K., Zhang, X.Y., Xiao, Y.K., 2010. Strontium and boron isotopic constraint on the marine origin of the Khammuane potash deposits in southeastern Laos. Chin. Sci. Bull. 55, 3181–3188.
Timofeeff, M.N., Lowenstein, T.K., Silva, M.A.M., Harris, N.B., 2006. Secular variation in the major-ion chemistry of seawater: evidence from fluid inclusion in Cretaceous halites. Geochim. Cosmochim. Acta 70, 1977–1994.
Titkov, S.N., 2004. Flotation of water-soluble mineral resources. Int. J. Miner. Process. 74, 107–113.
Utha-Aroon, C., 1993. Continental origin the Maha Sarakham evaporites, northeastern Thailand. J. SE Asian Earth Sci. 8, 193–203.

Valyashko, M.G., 1956. Geochemistry of bromine in the processes of salt deposition and the use of the bromine content as a genetic and prospecting criterion. Geochemistry 1 (6), 570–589.
Valyashko, M.G., Petrova, N.S., 1973. Experimental study of rubidium partitioning between sylvite crystals and solution in the NaCl–KCl–$MgCl_2$–H_2O system at 25 °C. Geokhimiya 4, 589–594.
Wardlaw, N.C., 1968. Carnallite-sylvite relationships in the Middle Devonian Prairie Evaporite Formation, Saskatchewan. Geol. Soc. Am. Bull. 79, 1273–1294.
Wardlaw, N.C., 1970. Effects of fusion, rates of crystallization and leaching on bromide and rubidium solid solutions in halite, sylvinite and carnallite. Third Symposium on Salt vol. 1. The Northern Ohio geological society, pp. 223–231.
Wardlaw, N.C., 1972. Unusual marine evaporites with salts of calcium and magnesium chloride in Cretaceous basins of Sergipe, Brazil. Econ. Geol. 67, 156–168.
Wardlaw, N.C., Watson, D.W., 1966. Middle Devonian salts formations and their bromide content, Elk Point area, Alberta. Can. J. Earth Sci. 3, 263–275.
Warren, K., 1999. Evaporites: Their Evolution and Economics. Oxford, Blackwell Science, pp. 235–239.
Weck, P.F., Kim, E., Jové-Colón, C.F., Sassani, D.C., 2014. First-principles study of anhydrite, polyhalite and carnallite. Chem. Phys. Lett. 594, 1–5.
Xia, S.P., Hong, X.L., Gao, S.Y., 1993. Study on the dissolution kinetics and mechanism of carnallite and KCl. J. Salt Lake Res. 1 (4), 52–60 (in Chinese with English abstract).
Yalamanchili, M.R., Kellar, J.J., Miller, J.D., 1993. Adsorption of collector colloids in the flotation of alkali halide particles. Int. J. Miner. Process. 39, 137–153.
Zhang, X.Y., Ma, H.Z., Ma, Y.Q., Tang, Q.L., Yuan, X.L., 2013. Origin of the late Cretaceous potash-bearing evaporites in the Vientiane Basin of Laos: $\delta^{11}B$ evidence from borates. J. Asian Earth Sci. 62, 812–818.
Zhang, X.Y., Cheng, H.D., Tan, H.B., Yuan, X.L., Li, Y.S., Miao, W.L., Li, T.W., Ma, H.Z., 2015. Late Cretaceous potash evaporites in Savannakhet basin of middle Laos: geochemical evidence of non-marine inputs. Acta Petrol. Sin. 31, 2783–2793 (in Chinese with English abstract).
Zherebtsova, I.K., Volkova, N.N., 1966. Experimental study of trace element behavior during natural evaporation of Black Sea water and Sasyk–Sivash brine. Geokhimiya 6, 832–845.